Japanese Journal of Radiology (2019) 37:500–510
https://doi.org/10.1007/s11604-019-00830-6

ORIGINAL ARTICLE

Ethanol fixation method for heart and lung imaging in micro-CT

Matej Patzelt[1,2,3] · Jana Mrzilkova[1,2,3] · Jan Dudak[1,2,4,5] · Frantisek Krejci[1,2,4] · Jan Zemlicka[1,2,4] · Jakub Karch[1,2,4,5] · Vladimir Musil[1,2,3,6] · Jozef Rosina[1,2,5,7] · Viktor Sykora[8] · Barbora Horehledova[9] · Petr Zach[1,2,3]

Received: 21 November 2018 / Accepted: 8 March 2019 / Published online: 14 March 2019

Abstract

Purpose The soft tissue imaging in micro-CT remains challenging due to its low intrinsic contrast. The aim of this study was to create a simple staining method omitting the usage of contrast agents for ex vivo soft tissue imaging in micro-CT.

Materials and methods Hearts and lungs from 30 mice were used. Twenty-seven organs were either fixed in 97% or 50% ethanol solution or in a series of ascending ethanol concentrations. Images were acquired after 72, 168 and 336 h on a custom-built micro-CT machine and compared to scans of three native samples.

Results Ethanol provided contrast enhancement in all evaluated fixations. Fixation in 97% ethanol resulted in contrast enhancement after 72 h; however, it caused hardening of the samples. Fixation in 50% ethanol provided contrast enhancement after 336 h, with milder hardening, compared to the 97% ethanol fixation, but the visualization of details was worse. The fixation in a series of ascending ethanol concentrations provided the most satisfactory results; all organs were visualized in great detail without tissue damage.

Conclusions Simple ethanol fixation improves the tissue contrast enhancement in micro-CT. The best results can be obtained with fixation of the soft tissue samples in a series of ascending ethanol concentrations.

Keywords Ethanol · Micro-CT · Mice · Heart · Lungs

✉ Jana Mrzilkova
jana.mrzilkova@lf3.cuni.cz

1 Specialized Laboratory of Experimental Imaging, Third Faculty of Medicine, Charles University, Prague, Czech Republic

2 Institute of Experimental and Applied Physics and Faculty of Biomedical Engineering, Czech Technical University in Prague, Prague, Czech Republic

3 Department of Anatomy, Third Faculty of Medicine, Charles University, Ruska 87, 100 34 Prague, Czech Republic

4 Institute of Experimental and Applied Physics, Czech Technical University in Prague, Prague, Czech Republic

5 Faculty of Biomedical Engineering, Czech Technical University in Prague, Kladno, Czech Republic

6 Centre of Scientific Information, Third Faculty of Medicine, Charles University, Prague, Czech Republic

7 Department of Medical Biophysics and Informatics, Third Faculty of Medicine, Charles University, Prague, Czech Republic

8 Center for Experimental Biomodels, First Faculty of Medicine, Charles University, Prague, Czech Republic

9 Department of Radiology and Nuclear Medicine, Maastricht University Medical Center, Maastricht, The Netherlands

Introduction

Microcomputed tomography (micro-CT) is identical in its basic principles to a medical CT [1]. It uses X-ray attenuation data acquired from multiple projection angles and provides non-destructive 3D information of the inner structures of the investigated organs or tissues [2, 3]. Although it is nowadays possible to perform in vivo micro-CT scans of small animals, ex vivo scans of individual inner organs achieve still much higher spatial resolution and, therefore, provide better information on fine anatomical structures. State-of-the-art micro-CT systems provide spatial resolution down to several micrometers or even with sub-micron resolution in the case of laboratory-scale devices or using synchrotron radiation, respectively. The contrast in micro-CT arises from the attenuation of X-rays by absorption or scattering processes in examined objects [4]. Typically, highly mineralized structures, such as bones or teeth, which contain calcium phosphate minerals, give very good contrast in micro-CT.

Conversely, imaging of soft tissues such as nerves, muscles, adipose tissue or ligaments is quite challenging [5].

It is mainly due to low intrinsic X-ray contrast of soft tissues, which contain mainly low-atomic-number elements (carbon, hydrogen, oxygen), so it is necessary to use X-ray-absorbing contrast agents [1]. During the past years, several staining methods have been developed to increase the contrast of soft tissue structures [6]. However, most of these methods are complicated, time-consuming and some even use toxic contrast agents. One of the best and most widely used contrast agents for soft tissue contrast enhancement is aqueous solutions of osmium tetroxide (OsO_4), phosphomolybdic acid (PMA) or phosphotungstic acid (PTA) [5]. OsO_4 is very toxic, does not stain well if samples have been in alcohol and also its penetration is relatively slow. PTA also penetrates the tissues slowly, but it is less toxic, simpler to use and stains effectively alcohol-stored samples [1]. PMA gives better contrast among different tissues, but requires longer incubation [6].

Currently, micro-CT imaging of the heart mainly focuses on depicting healthy or damaged coronary arteries. For ex vivo imaging, a radio-opaque polymer blend (Microfil) is injected into the heart vasculature [7] or the OsO_4 fixation of the heart is used [8]. In vivo studies of the vascular system of mice usually apply intravenous iodine contrast agent [9]. The heart was also visualized in studies of embryos, where either iodine staining [10, 11] or OsO_4 fixation was used [6].

Regarding lungs, current studies mainly focus on in vivo imaging of pathologically changed mice lungs, to capture longitudinal information about the progression of the illness in preclinical models [12, 13]. These studies mainly aim to image lung tumors, using contrast agents such as gold nanoparticles or liposomal iodine [14] or lung fibrosis [15]. The imaging of healthy lungs was performed in studies evaluating structural differences between different mouse phenotypes [16].

Regardless of the assessed organ, an ideal contrast agent should be easily administered and have the ability to equally penetrate through the thick tissue layers [17]. Ethanol, currently used as a medium for a conservation of the samples or as a liquid medium for samples during scanning, showed potential to fulfill these criteria [1]. Takeda et al. [18] used 100% ethanol perfusion in rat brain for contrast enhancement during micro-CT acquisition with phase-contrast X-ray technique. A 100% ethanol solution was also used in the study by Shirai et al. [19], for kidney imaging in phase-contrast X-ray computed tomography. To our best knowledge, there is no study using only pure ethanol as a contrast medium for X-ray imaging of soft tissue based on absorption contrast.

The aim of this study was to evaluate whether ethanol would be a suitable contrast agent for ex vivo staining of the heart and lungs prior to micro-CT imaging based on absorption contrast.

Materials and methods

Tissue sample origins

The organs of 30 C57BL/6 genetically modified male mice (weight 17–20 g) were harvested for the purpose of this study. Mice were killed by cervical dislocation under the halothane anesthesia. Use of laboratory animals was approved by the local Ethical Committee of First and Third Faculty of Medicine, Charles University, Prague, Czech Republic. The animals were treated in accordance with the guidelines defined by the ethical committee, which follows The National Advisory Committee for Laboratory Animal Research (NAC LAR) guidelines.

Tissue sample fixation

Three different ethanol fixation protocols were used. Nine specimens were fixed with either protocol A, B or C. Protocol A and B used ethanol solution with a fixed concentration of 97% or 50%, respectively. Protocol C consisted of four consequent ethanol baths, each with increasing ethanol concentrations in the solution. Samples were fixed in 12-h steps, using ethanol solutions with ascending concentrations of 25%, 50%, 75% and 97%, respectively. The expected outcome after immersion in ethanol was shrinkage of the specimens [2], which was supposed to be different in various types of fixations.

After the scanning was complete, we stored the samples for 6 months at a 4 °C environment to evaluate the long-term fixation effect on the specimens.

Hearts and lungs from 3 mice were carefully harvested and then put into phosphate-buffered saline (PBS solution) for 2 h and then scanned as native specimens. These organs served as a reference set of samples to the examined ethanol fixation protocols.

Tissue sample imaging

Each sample was scanned just once, to avoid distortion of the results due to changes of the specimen volume during scanning. The imaging was performed systematically after 72 h, 168 h and 336 h of fixation. The 72-h time point was chosen according to an experiment based on the basic protocols for histological processing of the samples. To investigate the effect of long-term ethanol fixation on the specimens, additional scans were performed at the 168- and 336-h time points.

Before the scanning, the fixed organs were placed on a gauze at an air temperature of 23 °C to dry. The optimal length of tissue drying period was determined with the

previous experiment, where the organs were scanned in 2 min intervals during the drying period. With increasing drying time, more details became visible in distal parts of the organ. A period of 40 min provided the best visualization of details in both heart and lungs, as it allowed the redundant ethanol to vaporize from the whole organ including the vessels, ventricles, and other cavities. These structures, normally filled with liquid, became hollow during this time, and, due to ethanol that caused tissue stiffness, the cavities did not collapse. The air-tissue transition then produces a detectable absorption contrast. When the drying period was completed, the organs were positioned in a dedicated plastic holder with an ethanol reservoir. This device provided a stable environment with ethanol vapor and thus prevented structural changes of the organs during imaging [20].

The imaging protocol was identical for the ethanol fixed and native specimens.

Two different consecutive imaging protocols were used. First, X-ray micro-radiography of each sample using 60 kVp unfiltered tungsten spectrum and with 22 µm effective pixel size (EPS) was performed. This acquisition resulted in a 2D projection. Second, a micro-CT acquisition using the same X-ray spectrum but with a resolution higher than 10 µm delivered a 3D reconstruction of the specimen.

The data were acquired with an emphasis on high CNR. Therefore, the acquisition time was individually adjusted to achieve at least 10^5 or 10^4 detected photons per pixel behind the object in the case of a micro-radiography or a micro-CT projection, respectively. Micro-CT datasets were acquired with a total of 720 projections with 0.25° angle step. The data were transformed from the intensity domain to equivalent material thickness using a beam hardening correction designed for photon-counting detectors (PCDs) [21]. CT reconstructions were performed using the Volex reconstruction engine (courtesy of Fraunhofer ISS and Technology, Germany).

All CT data were evaluated in CTVox software [22].

Volume and shrinkage measurements

The shrinkage of the specimens was counted from the measurements of the three dimensions (height, length, depth) of the specimens with a sliding scale. Additionally, the volume of the specimen was assessed following the methodology used by Vickerton et al. [2]. Briefly, the volume of the specimen was measured in the water-filled tube, according to the rise in the level of water. The native dimensions of the specimens were assessed immediately after explantation. Dimensions of the fixed samples were assessed at the end of the fixation period. Each measurement was repeated five times. The percentage of shrinkage was calculated from the change of the volume and the dimensions between native and fixed sample.

Histological processing

Each organ was also processed histologically, to compare non-destructive soft tissue visualization obtained from micro-CT with conventional histology.

Samples originally fixed with one of the ethanol fixation protocols were first put in a 10% formalin solution for 2 h at 37 °C. Second, a dehydration process in six baths of alcohol (97% alcohol–benzene) for a total of 6 h at 37 °C was carried out. Third, the samples were fixed with alcohol–xylene 1:1 solution for 1 h at 45 °C, followed by two baths in xylene, in total for 2 h at 45 °C. Fourth, the samples were put in three paraffin baths for 5 h at a temperature of 60 °C and embedded in paraffin blocks. Fifth, after cutting paraffin blocks into slices, these were rehydrated again. Lastly, slices were stained with hematoxylin–eosin and Weigert van Gieson staining method, before they could be evaluated under a standard light microscope and binocular magnifying glass.

Scoring of the contrast enhancement

For a quantitative comparison of the microradiographies, the contrast number was adopted from Pauwels et al. [17]. In hearts, the relative contrast difference between the right ventricle of the heart and its wall was calculated from the mean gray value in Pixelman Software (IEAP CTU Prague) [23]. It was calculated with a formula $C=(G_1-G_2)/G_1$, where G_1 represents the mean gray value of the right ventricle and G_2 is the mean gray value of the wall of the right ventricle.

The same process was done in the lungs, where contrast was calculated between the alveolar sac and its wall. The same formula was used, where G_1 is the mean gray value of the cavity of the alveolar sac and G_2 represents the mean gray value of the wall of the alveolar sac.

The mean gray values of all microradiographies were measured in raw data before BH corrections, selecting the region of interest (ROI). The contrast was then expressed in percentages.

In the scans of both the studied organs, monitored structures were set, in order to compare the quality of scans. Muscle fibers, left and right ventricle, left and right auricle, pectinate muscles, papillary muscles and aorta were set as monitored structures in the heart samples. Trachea, primary bronchus, lobar bronchus and alveolar sacs were set as monitored structures in lungs.

The subjective image quality was evaluated using a 4-point Likert scale: grade 1 = no monitored structures differentiation (contrast enhancement not sufficient for evaluation), grade 2 = possible to differentiate monitored structures (image sufficient for structure differentiation, although contrast enhancement is unsatisfactory), grade 3 = good (image with satisfactory contrast enhancement), grade 4 = excellent (image with optimal contrast enhancement).

Table 1 Summary of the shrinkage, calculated contrast and ruptures of the heart specimens

	Heart									
	Native	A (97%) 72 h	A (97%) 168 h	A (97%) 336 h	B (50%) 72 h	B (50%) 168 h	B (50%) 336 h	C (Asc.) 72 h	C (Asc.) 168 h	C (Asc.) 336 h
Shrinkage	No	21 ± 2%	21 ± 2%	21 ± 2%	14 ± 2%	14 ± 2%	14 ± 2%	18 ± 2%	18 ± 2%	18 ± 2%
Rupture of at least 1 specimen	No	Yes	Yes	Yes	No	No	No	No	No	No
Contrast between ventricle and muscles	12 ± 1%	29 ± 2%	34 ± 2%	31 ± 1%	14 ± 1%	20 ± 2%	24 ± 2%	30 ± 2%	36 ± 1%	33 ± 2%

Table 2 Summary of the shrinkage, contrast and ruptures of the lung specimens

	Lungs									
	Native	A (97%) 72 h	A (97%) 168 h	A (97%) 336 h	B (50%) 72 h	B (50%) 168 h	B (50%) 336 h	C (Asc.) 72 h	C (Asc.) 168 h	C (Asc.) 336 h
Shrinkage	No	18 ± 2%	18 ± 2%	18 ± 2%	12 ± 2%	12 ± 2%	12 ± 2%	15 ± 2%	15 ± 2%	15 ± 2%
Rupture of at least 1 specimen	No	Yes	Yes	Yes	No	No	No	No	No	No
Contrast between ventricle and muscles	15 ± 1%	18 ± 1%	23 ± 1%	20 ± 1%	16 ± 1%	20 ± 2%	24 ± 1%	28 ± 2%	33 ± 1%	36 ± 2%

Micro-CT apparatus

Two different custom-built micro-CT systems were used for purposes of this study. Both of them use cone-beam imaging geometry and a unique detector technology—Timepix photon-counting detectors (PCD) [24].

The basic Timepix assembly consists of a semiconductor sensor bump bonded to an electronic read-out chip composed of an array of 256 × 256 pixels with 55 µm pixel pitch. The significant advantage of the used PCD technology for low-contrast objects lies in a dark-current-free quantum-counting operation allowed by an adjustable energy threshold in each individual pixel. Thanks to these features, PCDs acquire noiseless data with virtually unlimited dynamic range. Therefore, an enormously high contrast-to-noise ratio (CNR) can be achieved. High CNR improves the detectability of low-contrast detail within the scanned object [25]. Although the pixel size of a Timepix device is 55 µm, it is possible to achieve much higher spatial resolution thanks to the cone-beam imaging geometry; point-like source of radiation produces a divergent beam of X-rays that magnifies the projection of a sample by a factor $M = \mathrm{SDD/SOD}$, where SDD is source–detector distance and SOD is source–object distance. In such case, ESP is commonly used to characterize the sampling density of the radiographic image. EPS is defined as the ratio between actual pixel size of the used detector and magnification factor M. Such an approach is generally used in the field of micro-CT for improving spatial resolution and detail detectability of the acquired data.

The first used system is equipped with a Kevex™ PXS-11 X-ray tube with focal spot size 28 µm and Timepix detector in Quad configuration (four read-out chips with a common silicon sensor providing a sensitive area 28 × 28 mm). The highest achievable spatial resolution is approx. 28 µm in this case. All presented 2D micro-radiographic images were acquired using the introduced setup [26].

The second system has been designed to provide a much higher spatial resolution and wide field of view. Thanks to a high-quality micro-focus X-ray tube Hamamatsu L8601-01 with focal spot size down to 5 µm, the setup achieves spatial resolution down to 5 µm [27]. It was recently upgraded by a large area Timepix detector built using WidePIX technology—a newly developed technique for assembling large area PCD arrays [28]. The used detector $\mathrm{WidePIX}_{10\times5}$ consists of 50 individual Timepix tiles and provides a field of view approx. 140 × 70 mm. The high-resolution setup was used for the presented micro-CT scans.

Statistical analysis

Statistical analysis was conducted using Statistical Package for Social Sciences version 23.0 (SPSS Inc., Chicago, IL, USA). One sample t test with a 2-sided α of 5% was used in this study. Continuous variables were expressed using mean values ± standard deviations (SD).

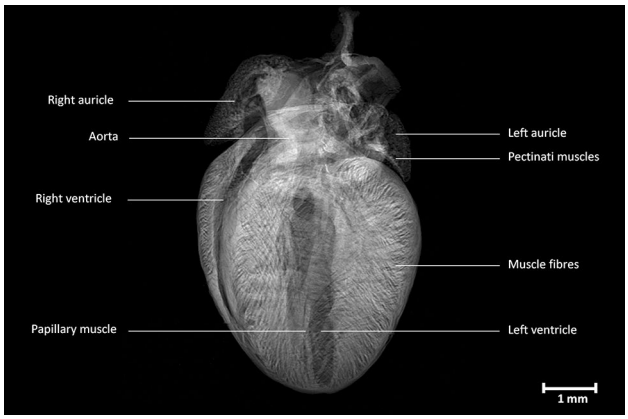

Fig. 1 High-resolution micro-radiography of a mouse heart. The heart was fixed in a series of ascending ethanol concentrations and scanned after 168 h

Results

All specimens were well fixed in ethanol; there was no sign of decomposition or rot. The quality of the tissue was not changed even after 6 months of fixation.

No scans were presented with *no monitored structures differentiation* (grade 1) or *possible to differentiate monitored structures* (grade 2). Scans of hearts and lungs fixed in 50% ethanol were scored as good (grade 3), and the rest of the scans were scored as excellent (grade 4).

The level of shrinkage, calculated contrast and also eventual rupture of the specimen are summarized in Tables 1 and 2.

Heart

Micro-radiography of a native specimen showed only the contour of the organ and no details of muscles, vessels or any other structures. As for the ethanol fixation, all evaluated fixation protocols yielded visualization of the heart in X-ray scan better compared to the native specimen. Micro-radiographs of fixed hearts depicted all monitored structures—muscle fibers, left and right ventricle, left and right auricle, pectinate muscles, papillary muscles and aorta (Fig. 1). The 3D reconstruction visualized the valves, tendinous cords and course of the muscles as heart's vortex and trabeculae, in addition to the basic structures visible on 2D micro-radiography.

In 97% ethanol fixation, the highest level of stiffness and shrinkage of the samples was observed. Due to very fast dehydration, small ruptures of the samples were observed in

two cases. Figure 2a shows a comparison of scans assessed after 72, 168 and 336 h of fixation and a native specimen.

Already after 72 h fixation, there was a significant contrast enhancement and all monitored structures were visible. The best visualization details within this ethanol concentration were, however, obtained after 168 h of fixation. Fixation for 336 h did not provide better visualization of the monitored structures or higher calculated contrast than 168 h of fixation.

With 50% ethanol fixation, all monitored structures were visualized. The sample was softer compared to the 97% ethanol protocol with no signs of rupture. Figure 2b shows a comparison of scans assessed after 72, 168 and 336 h of fixation and a native specimen.

The contrast enhancement after 72 h of fixation was only slightly better than in a native specimen. The best detailed visualization was observed after 336 h of fixation. However, fixation in 50% ethanol proved to be inferior to the 97% ethanol fixation protocol, in regard to sharp detail visualization.

The fixation in a series of ascending ethanol concentrations presented with a sample stiffness comparable to the 97% fixation protocol, but with no signs of specimen rupture. In all observed time points, a significant contrast enhancement was observed. According to calculated contrast, the best detailed visualization was reached after 168 h of fixation (Fig. 2c); however, the quality of visualization of the monitored structures was proportionate to the 72 h

Fig. 2 X-ray micro-radiography of a mouse heart, comparing a native heart (left) to the fixed hearts (the rest). **a** Fixed in 97% ethanol for 72, 168 and 336 h, **b** fixed in 50% ethanol for 72, 168 and 336 h, **c** fixed in a series of ascending ethanol concentrations for 72, 168 and 336 h

fixation protocol. Fixation for 336 h did not provide better contrast enhancement than 168 h of fixation.

Fixation in a series of ascending ethanol concentrations provided the best detailed morphological imaging of all monitored structures of the heart.

3D reconstruction in comparison to histological samples of the heart is shown in Fig. 3. It shows the comparison between 3D micro-CT reconstruction and histological processing of a mouse heart fixed in a series of ascending ethanol concentrations and scanned after 168 h of fixation. 3D reconstructions from micro-CT scans show more of inner structures of the heart in comparison to histological processing, which, however, yielded a better resolution.

Lungs

High-resolution X-ray radiography of a native specimen showed, due to natural air-tissue contrast, not only the contour of the organ, but also a primary bronchus and its first branching. X-ray micro-radiography of fixed lungs revealed all monitored structures—trachea, primary bronchus, lobar bronchus and alveolar sacs (Fig. 4). The 3D reconstruction visualized the carina of the trachea, margins of pulmonary lobes and peripheral branching of the primary bronchus, in addition to the basic structures visualized on X-ray micro-radiography images.

The 97% ethanol fixation protocol caused significant stiffness, shrinkage and even tissue deformation of all samples. Figure 5a shows a comparison of contrast improvement in organs fixed in ethanol (72, 168 and 336 h) and in the native specimen.

After 72 h fixation, the contrast between the alveolar sac and its wall was $18 \pm 1\%$. All monitored structured were visible. After 168 h of fixation, the best detailed visualization of all monitored structures was achieved, even with sharp details of the peripheral alveolar sacs. The fixation for 336 h provided a comparable visualization of the monitored structures as 168 h fixation protocol.

In 50% ethanol fixation, all monitored structures were visible. There was also a stiffness and shrinkage of the samples, although not that severe as with 97% concentration. There were no signs of specimen rupture. The 72 h fixation did not significantly increase the contrast between the alveolar sac and its wall compared to the native specimen.

The best detailed visualization was according to calculated contrast after 336 h of fixation; however, the contrast was only $24 \pm 1\%$, which was essentially the same as after 168 h of fixation with 97% ethanol fixation protocol. The depiction of sharp details was inferior compared to the 97% fixation protocol (Fig. 5b).

The fixation in a series of ascending ethanol concentrations presented with a stiffness of the sample, similar to the 97% ethanol fixation protocol. In all assessed time points,

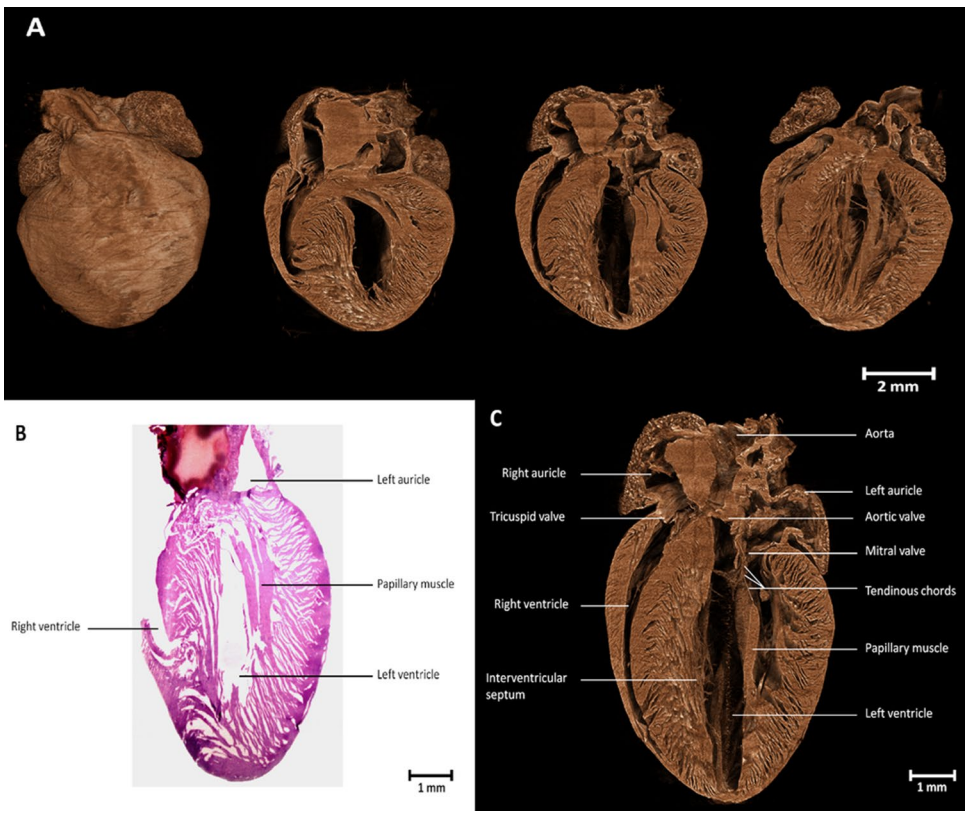

Fig. 3 Comparison between micro-CT imaging and histological processing of a mouse heart. **a** 3D micro-CT reconstruction of a mouse heart fixed in a series of ascending ethanol concentrations and scanned after 168 h; data acquired with 7.2 µm EPS. **b** Histological sample of the same mouse heart, performed after scanning in micro-CT; the sample was stained with hematoxylin–eosin. **c** 3D reconstruction of a mouse heart fixed in a series of ascending ethanol concentrations and scanned after 168 h

Fig. 4 X-ray micro-radiography of mouse lungs. The lungs were fixed in a series of ascending ethanol concentrations and scanned after 336 h

there was a significant contrast enhancement and adequate visualization of all monitored structures. The best detailed visualization was depicted after 336 h of fixation (Fig. 5c).

The 336 h fixation in a series of ascending ethanol concentrations provided the best detailed morphological imaging of lung structures compared to other fixation protocols.

3D reconstruction in comparison to the histological samples of the lungs is shown in Fig. 6. It has a quality between 3D X-ray micro-CT reconstruction and histological processing of mouse lungs. 3D reconstruction from micro-CT scan shows more of its inner structure; conversely, histological processing reached a better resolution.

Discussion

Soft tissue imaging with micro-CT is generally challenging due to the low intrinsic contrast of soft tissue in organs. Although several staining techniques for ex vivo use were introduced in the past years, most of these methods proved to be complicated, time-consuming and in some cases even toxic. This study clearly shows that ethanol solution can be used as a simple, cheap and stable fixation method dedicated to ex vivo soft tissue fixation prior to micro-CT imaging, while delivering improved contrast enhancement of soft tissues in organs.

We compared ethanol fixation protocols, which vary in ethanol concentration of the ethanol and in the duration of fixation. All ethanol fixation protocols used in the current study enhanced the contrast in mouse heart and lungs and provided detailed morphological information about the inner structure of these organs. Within the mouse heart, we were able to distinguish delicate structures such as the valves or tendinous cords. In the mouse lungs, even the alveoli structures were well visualized. The inner structure visualization was the main imaging drawback in the methods introduced by Descamps et al. [6], who tested OsO_4, PMA and PTA for discrimination between tissue types and organs. They managed to beautifully distinguish individual organs in embryos; however, a detailed inner structure of these organs was missing. Besides other disadvantages, OsO_4 and PTA are toxic agents and PMA requires long incubation.

PTA and OsO_4 together with inorganic iodine were also evaluated in the study by Metscher et al. [1]. Inorganic iodine is a well-known staining agent for micro-CT; it provides very good contrast among the tissues and rapidly diffuses into the specimen. The results of our current study raise question whether the ethanol solution has effect on inorganic iodine contrast enhancement or not. This is a topic for a next study.

The principle of our method is quite simple. Ethanol causes protein denaturation through the removal of the water molecule from the free carboxyl, hydroxyl, amino,

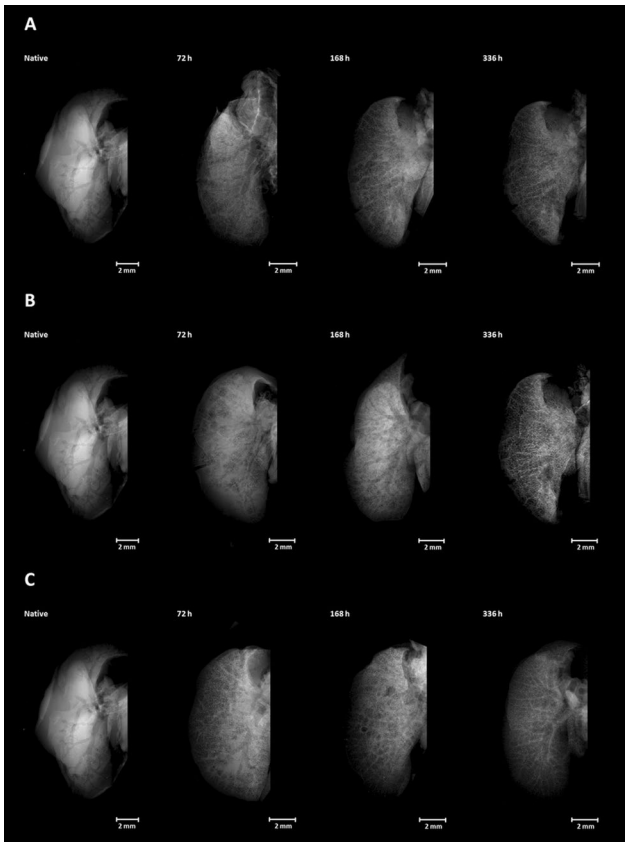

Fig. 5 X-ray micro-radiography of a mouse right lung, comparing a native right lung (left) to the fixed right lungs (the rest). **a** Fixed in 97% ethanol for 72, 168 and 336 h, **b** fixed in 50% ethanol for 72, 168 and 336 h, **c** fixed in a series of ascending ethanol concentrations and scanned after 72, 168 and 336 h

amido and imino groups of the proteins, resulting in protein coagulation and tissue shrinkage [29]. Additionally, ethanol also increases the organs' stiffness. The organ cavities and hollow spaces, therefore, do not collapse, and the air-tissue transition then produces a detectable contrast. For that reason, ethanol fixation together with a photon-counting detector provides a detailed soft tissue discrimination in the studied organs.

The great advantage lies in the noninvasive nature of this method. After the scanning is completed, tissues are still available for further staining, histochemical procedures, or classical histology. Compared to histology, our method is much simpler and also does not require slicing of the sample and consequently its destruction.

Long-term fixation of the samples in ethanol, in this study 6 months, does not have any effect on the quality of the specimens. It is, therefore, possible to scan them on several occasions, also on different micro-CT machines or in various laboratories. Owing to the simplicity of this method, there are no special requirements for qualification

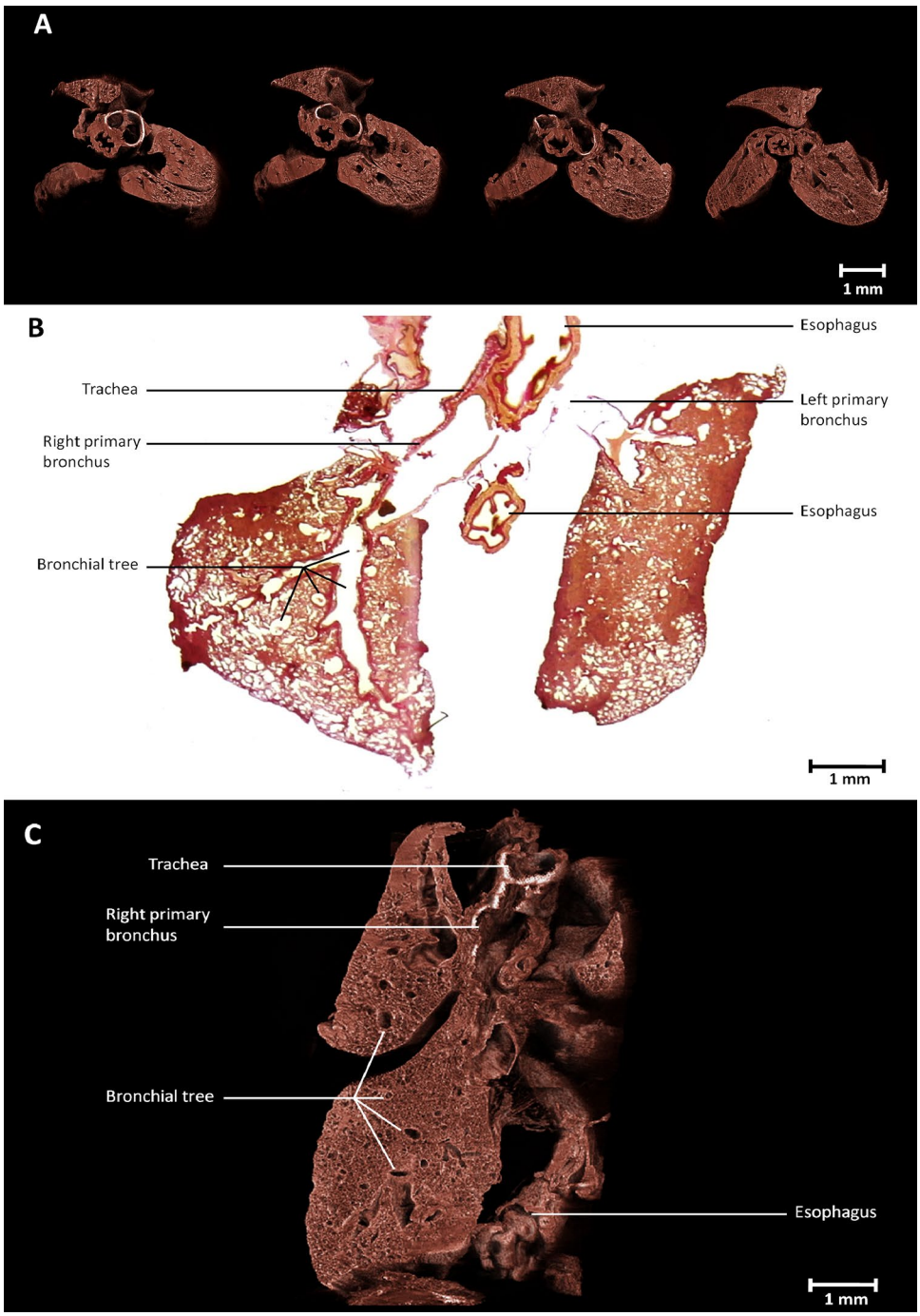

Fig. 6 Comparison between micro-CT imaging and histological processing of a mouse lung. **a** Transversal craniocaudal sections of 3D reconstruction of mouse lungs fixed in a series of ascending ethanol concentrations and scanned after 336 h, showing bifurcation of the trachea to primary bronchi and their topographical relationship to the esophagus, **b** histological sample of mouse lungs stained by Weigert van Gieson, **c** 3D reconstruction of mouse right lung, sagittal view; data acquired with EPS 3.55 µm

of laboratory personnel or laboratory equipment. This allows closer cooperation between researchers and laboratory personnel with different fields of expertise, or even use of this method by clinicians, who can collect the samples and simply fix them in a cartridge with the selected ethanol solution.

Furthermore, the 3D reconstructions can be easily and expeditiously analyzed in any cross sections with multiple post-procedural options, such as creating of rotational images or animations.

Possibly the fixation in 25% ethanol could be avoided, which could also reduce the duration of fixation time in each bath. However, optimal fixation times, number of baths and their concentrations in an ascending ethanol concentration protocol need to be determined with further study.

We believe that even more detailed structure imaging of tissue structures is possible with our ethanol protocol; however, it is currently limited by the spatial resolution of micro-CT machines. Although this research did not focus on pathological specimens, our protocol can be equally applied to pathological samples to depict morphological changes in organs.

The major limitation of this method is shrinkage of the soft tissue specimens, which was due to the properties of ethanol and it is technically unavoidable.

A relatively small number of specimens was evaluated per group. Only ethanol fixation methods were carried out in the current study, and comparison to conventional methods is therefore not available. However, a gold standard staining method is non-existent and a correlation to a reference measurement is not possible.

Conclusions

Ethanol fixation is a cheap and simple method, which can be used not only for the fixation of the soft tissue specimens, but also for tissue contrast enhancement in micro-CT imaging. The best results can be achieved when soft tissue fixation in a series of ascending ethanol concentrations is carried out.

Funding The work was supported by the Charles University Grant Agency [GAUK 130 717] and from European Regional Development Fund-Project “Engineering applications of microworld physics” [No. CZ.02.1.01/0.0/0.0/16_019/0000766].

Compliance with ethical standards

Conflicts of interest The authors declare that there is no conflict of interest regarding the publication of this paper.

Ethical statement All applicable institutional and national guidelines for the care and use of animals were followed.

References

1. Metscher BD. MicroCT for comparative morphology: simple staining methods allow high-contrast 3D imaging of diverse non-mineralized animal tissues. BMC Physiol. 2009;9:11. https://doi.org/10.1186/1472-6793-9-11.
2. Vickerton P, Jarvis J, Jeffery N. Concentration-dependent specimen shrinkage in iodine-enhanced microCT. J Anat. 2013;223(2):185–93. https://doi.org/10.1111/joa.12068.
3. Silva JMDE, Zanette I, Noel PB, Cardoso MB, Kimm MA, Pfeiffer F. Three-dimensional non-destructive soft-tissue visualization with X-ray staining micro-tomography. Sci Rep-UK. 2015;5:Artn 14088. https://doi.org/10.1038/srep14088.
4. Donath T, Pfeiffer F, Bunk O, Grunzweig C, Hempel E, Popescu S, et al. Toward clinical X-ray phase-contrast CT demonstration of enhanced soft-tissue contrast in human specimen. Invest Radiol. 2010;45(7):445–52. https://doi.org/10.1097/RLI.0b013e3181e21866.
5. Mizutani R, Suzuki Y. X-ray microtomography in biology. Micron. 2012;43(2–3):104–15. https://doi.org/10.1016/j.micron.2011.10.002.
6. Descamps E, Sochacka A, De Kegel B, Van Loo D, Van Hoorebeke L, Adriaens D. Soft tissue discrimination with contrast agents using micro-CT scanning. Belg J Zool. 2014;144(1):20–40.
7. Clauss SB, Walker DL, Kirby ML, Schimel D, Lo CW. Patterning of coronary arteries in wildtype and connexin43 knockout mice. Dev Dyn. 2006;235(10):2786–94. https://doi.org/10.1002/dvdy.20887.
8. Pai VM, Kozlowski M, Donahue D, Miller E, Xiao XH, Chen MY, et al. Coronary artery wall imaging in mice using osmium tetroxide and micro-computed tomography (micro-CT). J Anat. 2012;220(5):514–24. https://doi.org/10.1111/j.1469-7580.2012.01483.x.
9. Yamashita T, Kawashima S, Ozaki M, Namiki M, Hirase T, Inoue N, et al. Mouse coronary angiograph using synchrotron radiation microangiography. Circulation. 2002;105(2):E3–4. https://doi.org/10.1161/hc0202.100423.
10. Degenhardt K, Wright AC, Horng D, Padmanabhan A, Epstein JA. Rapid 3D phenotyping of cardiovascular development in mouse embryos by micro-CT with iodine staining. Circ Cardiovasc Imaging. 2010;3(3):314–22. https://doi.org/10.1161/Circimaging.109.918482.
11. Wong MD, Spring S, Henkelman RM. Structural stabilization of tissue for embryo phenotyping using micro-CT with iodine staining. PLoS ONE. 2013;8(12):e84321. https://doi.org/10.1371/journal.pone.0084321.
12. Gammon ST, Foje N, Brewer EM, Owers E, Downs CA, Budde MD, et al. Preclinical anatomical, molecular, and functional imaging of the lung with multiple modalities. Am J Physiol Lung C. 2014;306(10):L897–914. https://doi.org/10.1152/ajplung.00007.2014.
13. Vande Velde G, Poelmans J, De Langhe E, Hillen A, Vanoirbeek J, Himmelreich U, et al. Longitudinal micro-CT provides biomarkers of lung disease that can be used to assess the effect of therapy in preclinical mouse models, and reveal compensatory changes in lung volume. Dis Model Mech. 2016;9(1):91–8. https://doi.org/10.1242/dmm.020321.

14. Ashton JR, Clark DP, Moding EJ, Ghaghada K, Kirsch DG, West JL, et al. Dual-energy micro-CT functional imaging of primary lung cancer in mice using gold and iodine nanoparticle contrast agents: a validation study. PLoS ONE. 2014;9(2):e88129. https://doi.org/10.1371/journal.pone.0088129.
15. Rodt T, von Falck C, Dettmer S, Halter R, Maus R, Ask K, et al. Micro-computed tomography of pulmonary fibrosis in mice induced by adenoviral gene transfer of biologically active transforming growth factor-beta 1. Resp Res. 2010;11:181. https://doi.org/10.1186/1465-9921-11-181.
16. Thiesse J, Namati E, Sieren JC, Smith AR, Reinhardt JM, Hoffman EA, et al. Lung structure phenotype variation in inbred mouse strains revealed through in vivo micro-CT imaging. J Appl Physiol. 2010;109(6):1960–8. https://doi.org/10.1152/japplphysiol.01322.2009.
17. Pauwels E, Van Loo D, Cornillie P, Brabant L, Van Hoorebeke L. An exploratory study of contrast agents for soft tissue visualization by means of high resolution X-ray computed tomography imaging. J Microsc-Oxf. 2013;250(1):21–31. https://doi.org/10.1111/jmi.12013.
18. Takeda T, Thet-Thet-Lwin Kunii T, Sirai R, Ohizumi T, Maruyama H, et al. Ethanol fixed brain imaging by phase-contrast X-ray technique. J Phys: Conf Ser. 2013;425:022004. https://doi.org/10.1088/1742-6596/425/2/022004.
19. Shirai R, Kunii T, Yoneyama A, Ooizumi T, Maruyama H, Lwin TT, et al. Enhanced renal image contrast by ethanol fixation in phase-contrast X-ray computed tomography. J Synchrotron Radiat. 2014;21(Pt 4):795–800. https://doi.org/10.1107/S1600577514010558.
20. Dudak J, Zemlicka J, Krejci F, Karch J, Patzelt M, Zach P, et al. Evaluation of sample holders designed for long-lasting X-ray micro-tomographic scans of ex vivo soft tissue samples. J Instrum. 2016;11:C03005. https://doi.org/10.1088/1748-0221/11/03/C03005.
21. Jakubek J. Data processing and image reconstruction methods for pixel detectors. Nucl Instrum Methods A. 2007;576(1):223–34. https://doi.org/10.1016/j.nima.2007.01.157.
22. Bruker. CTVox: Volume Rendering [computer software] http://bruker-microct.com/products/downloads.htm (2015).
23. Turecek D, Holy T, Jakubek J, Pospisil S, Vykydal Z. Pixelman: a multi-platform data acquisition and processing software package for Medipix2, Timepix and Medipix3 detectors. J Instrum. 2011;6:C01046. https://doi.org/10.1088/1748-0221/6/01/C01046.
24. Llopart X, Ballabriga R, Campbell M, Tlustos L, Wong W. Timepix, a 65k programmable pixel readout chip for arrival time, energy and/or photon counting measurements. Nucl Instrum Methods A. 2007;581(1–2):485–94. https://doi.org/10.1016/j.nima.2007.08.079.
25. Dudak J, Zemlicka J, Karch J, Patzelt M, Mrzilkova J, Zach P, et al. High-contrast X-ray micro-radiography and micro-CT of ex vivo soft tissue murine organs utilizing ethanol fixation and large area photon-counting detector. Sci Rep-UK. 2016;6:30385. https://doi.org/10.1038/Srep30385.
26. Dudak J, Zemlicka J, Krejci F, Polansky S, Jakubek J, Mrzilkova J, et al. X-ray micro-CT scanner for small animal imaging based on Timepix detector technology. Nucl Instrum Methods A. 2015;773:81–6. https://doi.org/10.1016/j.nima.2014.10.076.
27. Jakubek J, Holy T, Jakubek M, Vavrik D, Vykydal Z. Experimental system for high resolution X-ray transmission radiography. Nucl Instrum Methods A. 2006;563(1):278–81. https://doi.org/10.1016/j.nima.2006.01.033.
28. Jakubek J, Jakubek M, Platkevic M, Soukup P, Turecek D, Sykora V, et al. Large area pixel detector WIDEPIX with full area sensitivity composed of 100 Timepix assemblies with edgeless sensors. J Instrum. 2014;9:C04018. https://doi.org/10.1088/1748-0221/9/04/C04018.
29. Howat WJ, Wilson BA. Tissue fixation and the effect of molecular fixatives on downstream staining procedures. Methods. 2014;70(1):12–9. https://doi.org/10.1016/j.ymeth.2014.01.022.